Available online at www.sciencedirect.com

SciVerse ScienceDirect

Ceramics International 39 (2013) 4399–4405

CERAMICS INTERNATIONAL

www.elsevier.com/locate/ceramint

Microstructure and hydrogen storage properties of MgH_2–TiB_2–SiC composites

Igor Milanović[a], Sanja Milošević[a], Željka Rašković-Lovre[a], Nikola Novaković[b], Radojka Vujasin[a], Ljiljana Matović[a], Jose Francisco Fernández[c], Carlos Sánchez[c], Jasmina Grbović Novaković[a,*]

[a]Vinča Institute of Nuclear Sciences, University of Belgrade, Department of Materials Science, P.O. Box 522, 11000 Belgrade, Serbia
[b]Vinča Institute of Nuclear Sciences, University of Belgrade, Department of Nuclear and Plasma Physics, P.O. Box 522, 11000 Belgrade, Serbia
[c]Departamento de Fisica de Materiales C-IV, Facultad de Ciencias, Universidad Autonoma de Madrid, Cantoblanco, 28049 Madrid, Spain

Received 14 September 2012; received in revised form 8 October 2012; accepted 13 November 2012
Available online 20 November 2012

Abstract

The influence of TiB_2 and SiC ceramics on H-desorption kinetics from MgH_2 based composites was investigated and correlated with the microstructure and morphology of the composites. The mechanism of desorption and the activation energy for desorption was investigated by applying non-isothermal kinetic analysis of thermodesorption spectra. It has been shown that TiB_2 addition leads to significant decrease of the activation energy for desorption, while SiC addition has effect on the interface reaction between hydride and hydroxide. The mechanism of desorption change from Avrami–Erofeev $n=3$ for pure MgH_2 to Avrami–Erofeev $n=4$ for composite materials. The change from 3 to 4 can be due to the modification of the nucleation process or a change in the dimensionality of the growth. Those high values of n discard a diffusion control as a rate limiting step.

Keywords: Mechanical milling; Composites MgH_2–TiB_2–SiC; Hydrogen storage; Kinetics

1. Introduction

Although hydrogen is an ideal energy carrier, there are still substantial technological challenges which hinder its use as a fuel. The development of safe, non-expensive and lightweight storage material is one of the major tasks for a future hydrogen technology, for both mobile and stationary applications. Hydrogen storage in lightweight metals or compounds is considered as the most promising method for a solid state storage. The solid state bonding of hydrogen in metals provides several advantages: high hydrogen density, which is ideal for transportation, there is no risk of leakage or explosion and finally, the hydrogen retained by this method has high purity, which is essential for its utilization in the fuel cells.

Among the metal hydrides, magnesium hydride is one of the most investigated materials owing to the fact that MgH_2 has high gravimetric density of hydrogen (7.6 wt%) [1]. However, slow sorption reaction rate is a major problem to solve, several methods of the lattice destabilization have been proposed: use of ion irradiation to introduce structural defects and strain in hydride lattice [2,3]; decrease of crystallite size of composite to nanoscale through mechanical milling [4–6], use of suitable oxide and non-oxide additives or catalysts together with mechanical milling [7–12].

Metal oxides are both catalysts and very efficient milling agents that can create defects in magnesium hydride structure due to their ceramic nature and ability to produce small grain size [9]. Because of their brittleness, the distribution of metal oxides in hydride matrix is quite homogeneous. They can also improve desorption kinetics even if they are added in very small doses [13,14].

Non-oxide ceramics such as SiC, TiC, TiB_2 also facilitate the rupture of MgH_2 particles and consequently reduce the

*Corresponding author. Tel.: +381 11 3408 552; fax: +381 11 3408 224.
E-mail address: jasnag@vinca.rs (J. Grbović Novaković).

0272-8842/$ - see front matter © 2012 Elsevier Ltd and Techna Group S.r.l. All rights reserved.
http://dx.doi.org/10.1016/j.ceramint.2012.11.029

particle size and increase the specific surface area [15–18]. Superior hydrogen storage properties of MgH_2–TiC have been reported by Fan et al. [19]. They have observed that composite releases 6.3 wt% of hydrogen at 573 K. Furthermore, halide additives milled with magnesium hydride reveal a strong catalytic influence on T_{onset} and T_{peak} of MgH_2 decomposition. The influence of TiB_2 on hydrogen desorption from MgH_2 has already been observed [11,20,21] and maximum temperature decrease of hydride decomposition was found to be 60 °C. Also, TiB_2 is known to be an excellent candidate for hydrogen storage by itself [22].

Even though the desorption temperature is decreased, the problem of rate limiting step still remains unresolved, since the general mechanism of (de)hydriding reaction can be described by several steps and any of them could be rate limiting [23].

To understand the kinetic and thermodynamic properties of MgH_2 based composites, thermal stability of MgH_2–TiB_2–SiC and MgH_2–TiB_2 powders was studied, employing the method of thermodesorption spectroscopy (TDS). Microstructure of the initial powder mixture and obtained composites was studied by scanning electron microscopy (SEM). X-ray powder diffraction analysis (XRD) was used to identify crystalline phases, lattice parameters, as well as crystalline size and strain, while particle size of composites was obtained using laser scattering method (PSD).

2. Experimental part

Tetragonal MgH_2 powder (Alfa Aesar, 98%) with average particle size of 38 μm, cubic β-SiC (B10 Hermann C. Starck) with average particle size of 31 μm [15] and hexagonal TiB_2 (Hermann C. Starck) with average size of 10 μm have been milled in high energy Turbula Type 2TC Mixer mill under argon atmosphere for 10 h, using ball to powder ratio of 10:1. The starting composition and nomenclature of obtained materials are given in Table 1.

Microstructural and morphological characterization of obtained composites was done by XRD analysis using Siemens Kristallflex D-500. The crystallite size and strain as well as phase composition of samples were calculated using the PowderCell 2.3 software [24]. Pseudo-Voigt (pV) function was selected to refine peak profile. Volume particle size distribution (PSD) is obtained by Mastersizer 2000SM, while SEM analysis was done using scanning electron microscope VEGA TS 5130MM, Tescan Brno.

Table 1
Chemical composition of synthesized material.

Sample	MgH_2 (wt%)	TiB_2 (wt%)	SiC (wt%)
AA	100	–	–
TiB5	95	5	–
TiB045	95	4.5	0.5
TiB005	95	0.5	4.5

Thermal desorption behavior of composites was followed in a combined DSC–TDS apparatus [25]. In this system the H_2 desorbed from the sample during non-isothermal conditions (heating rate of 5 K min^{-1} in temperature range 50–550 °C) was carried by an Ar flow (40 sccm min^{-1}) to a vacuum chamber. The quantitative analyses of H_2 desorbed from the samples were carried out using a quadrupole mass spectrometer type QMS 200 Balzers. Calibration of the spectrometer was performed with commercial MgH_2. More information about the experimental settings can be found elsewhere [25]. To obtain kinetics information of the H-desorption from the materials, non-isothermal numerical fitting of experimental data were used as explained in [23,26,27].

3. Results and discussion

3.1. Microstructure of material

X-ray diffractograms of commercial, non-treated MgH_2 (AA) and milled composite materials are presented in Fig. 1. It can be seen that the mechanical milling of MgH_2 with additives led to broadening of typical tetragonal β-MgH_2 peaks. The XRD patterns of the composites show additional peaks corresponding to TiB_2 and SiC. The broadening of XRD patterns indicates that there is a change in crystallite size and strain. The results of crystallite size reduction and increase of microstrain are presented in Table 2.

It was found that the crystallite size of β-MgH_2 has been decreased during milling with TiB_2 and SiC (see Table 2). This is a well known fact which can be ascribed to the creation of dislocations [28]. Since the observed MgH_2 peaks positions are slightly moved from database positions, there is an expansion of MgH_2 unit cell and therefore a possibility of non-stoichiometric MgH_2 phase

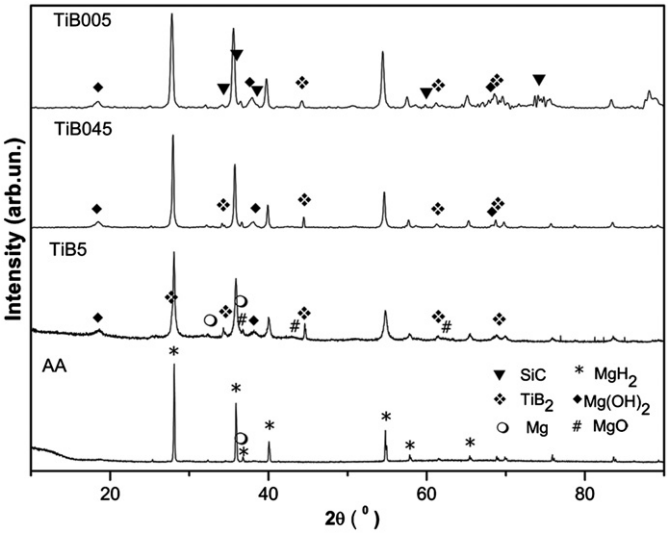

Fig. 1. XRD patterns of commercial, non-treated MgH_2 (AA) and mechanically milled composites: TiB5: 95% MgH_2–5% TiB_2; TiB045: 95% MgH_2–4.5% TiB_2–0.5% SiC and TiB045: 95% MgH_2–0.5% TiB_2–4.5% SiC.

Table 2
Crystallite size and microstrain of commercial, non-treated MgH_2 (AA) and mechanically milled composites TiB5, TiB045 and TiB005 obtained by refinement of XRD data by the PowderCell 2.3 software.

Sample	Crystallite size (nm)	Microstrain $\times 10^{-3}$ (%)	Lattice parameters and volume of MgH_2		
			a (Å)	c (Å)	V (Å^3)
AA	83	1.4	4.5168	3.0205	61.62
TiB5	41	2.5	4.5209	3.0206	61.73
TiB045	48	1.4	4.5179	3.0215	61.67
TiB005	29	0.6	4.5212	3.0266	61.86

Table 3
Phase composition of commercial, non-treated MgH_2 (AA) and mechanically milled composites TiB5, TiB045 and TiB005 obtained by refinement of XRD data by PowderCell 2.3 software.

Phases (wt%)	AA	TiB5	TiB005	TiB045
MgH_2	96	86.70	81.45	82.04
$Mg(OH)_2$	0.6	7.85	12.86	12.58
Mg	3.4	1.54	1.25	1.85
MgO	–	1.11	0.48	1.20
TiB_2	–	2.81	1.43	2.33
SiC	–	–	2.52	<1

formation [29,2] that could influence the kinetics of MgH_2 desorption.

Observed high quantities of $Mg(OH)_2$ result from the air exposure during the experiment. Although, milling was performed in Ar atmosphere, the oxide attached to the vial and the balls cannot be avoided and pure magnesium present in the starting powder is easily reduced to MgO and $Mg(OH)_2$ [2,3]. After milling, the powder is highly reactive because of energy transfer during collisions and it easily captures H_2O molecules from the air moisture producing $Mg(OH)_2$. It was observed that SiC addition increases the quantity of hydroxide. The ratio between phases in obtained composites is given in Table 3.

As can be seen from particle size distribution curves, the composites exhibit polymodal distribution (see Fig. 2). Regarding the composite TiB5 (dot line), more than 70% of particles have the particle size ranging from 1 to 10 μm, while 30% of particles have particles less than 1 μm. However, there are also agglomerates of about 100 μm (see SEM analysis, Fig. 3b). When SiC is added to the composite there is considerable increase of particles with size smaller than 1 μm (12% for composite TiB005 (solid line) and 6% for composite TiB045 (dashed line)). Further, there is a noticeable increase of particles with size ranging from 1 to 10 μm (52% for composite TiB005 (solid line) and 32% for composite TiB045 (dashed line)). This considerable decrease can be attributed to the addition of SiC [15] even though both SiC and TiB_2 has similar Mohs hardness (9–9.5). The average particle size of all samples is given in Table 4. Although, the average particle size is the lowest for the sample catalyzed only with TiB_2, the desorption temperature of this composite is higher than in systems catalyzed with SiC (see Section 3.2).

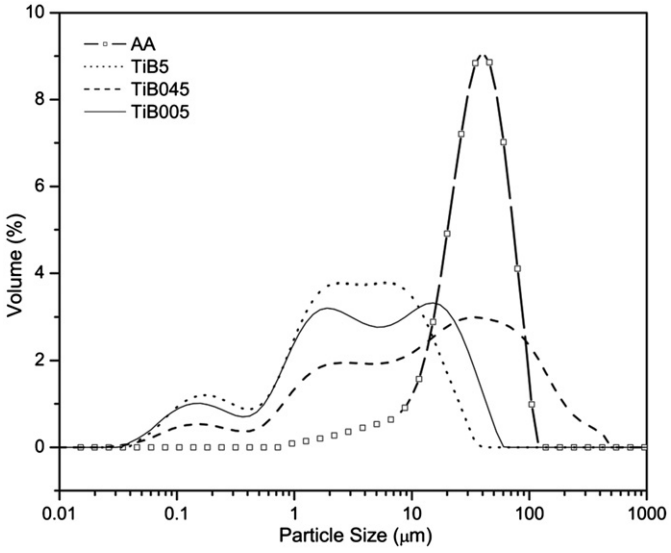

Fig. 2. PSD of commercial, non-treated MgH_2 (AA) and mechanically milled composite: TiB5 (dot line), TiB045 (dashed line) and TiB005 (solid line). The chemical composition of composite is given in Table 1.

According to several authors, the decrease of particle size is responsible for improved desorption properties of MgH_2 based materials and changed kinetics [2,11,18,28].

SEM micrographs (Fig. 3a) shows that the TiB_2 agglomerates have smooth surface and irregular shape with size ranging from 1 to 10 μm (confirmed by PSD). The layered structure is also noticeable. On the other hand, flaked MgH_2 particles [10] undergone to the significant changes due to intensive milling with TiB_2 (Fig. 3b). Noteworthy, the noticeable quantity of nanosize particles with sponge-like structure was formed, but large agglomerates are still visible. Milling with SiC as additive further changes the microstructure since large quantity of small sponge-like particles occur in both observed samples (Fig. 3c and d) [15]. It originates from $Mg(OH)_2$, accordingly to its higher concentration, as can be seen from XRD patterns in Fig. 1. Observed microstructural characteristics significantly change the properties of the system.

3.2. Desorption behavior of samples

Desorption behavior of non-treated MgH_2 (AA) and mechanically milled composite materials was examined by

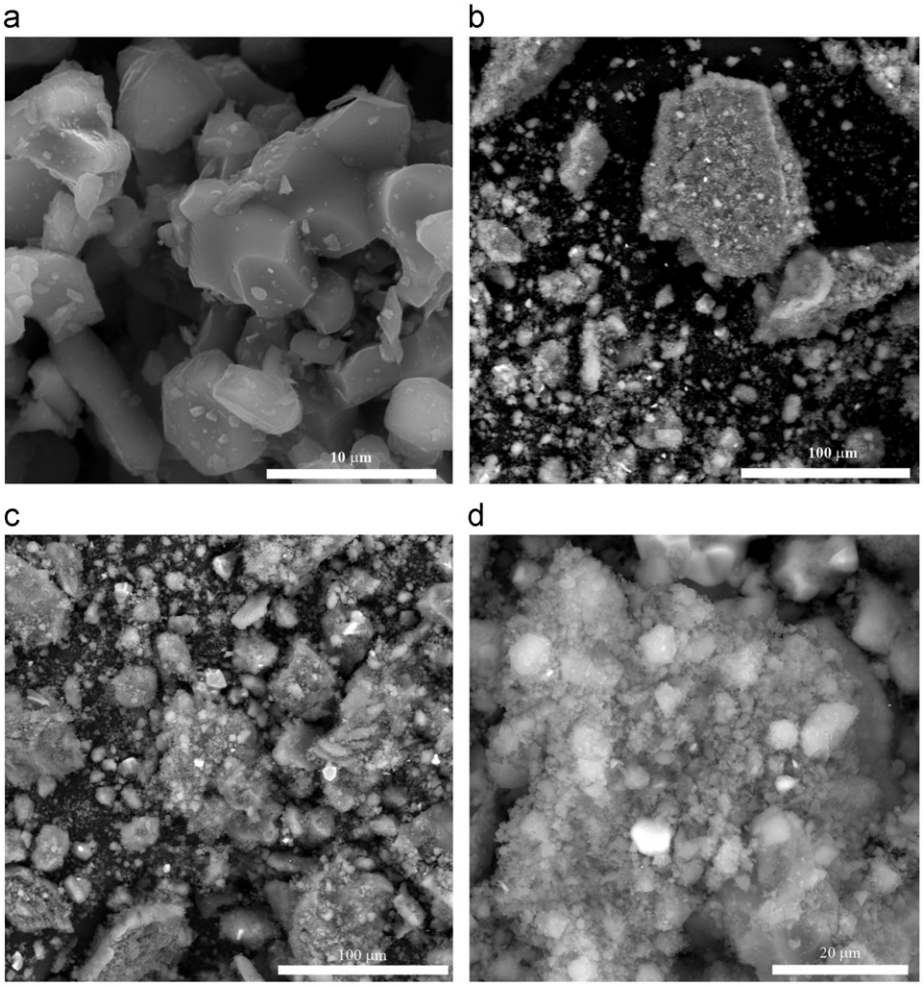

Fig. 3. SEM micrographs of pure TiB_2 (a) and mechanically milled composite materials: TiB5 (b), TiB005 (c) and TiB045 (d). The chemical composition of obtained composites is given in Table 1.

Table 4
Average particle size of all samples obtained from PSD analysis.

Sample	Average particle size		
	LV (μm)*	IV (μm)*	HV (μm)[a]
AA	–	–	38
TiB5	0.181	4	10
TiB045	0.120	0.166	17
TiB005	0.120	0.166	36

[a]LV—small particle size, IV—intermediate particle size, HV—coarse particles.

thermodesorption spectroscopy (TDS) and is presented in Fig. 4. All studied materials exhibited three desorption maxima, similar to those obtained in the literature [15,23,30]. Hydrogen release from the sample AA is visible at 450 °C (high temperature peak, HT-H_2), 350 °C the intermediate temperature peak, (IT-H_2) and at 180 °C, low temperature peak, LT-H_2.

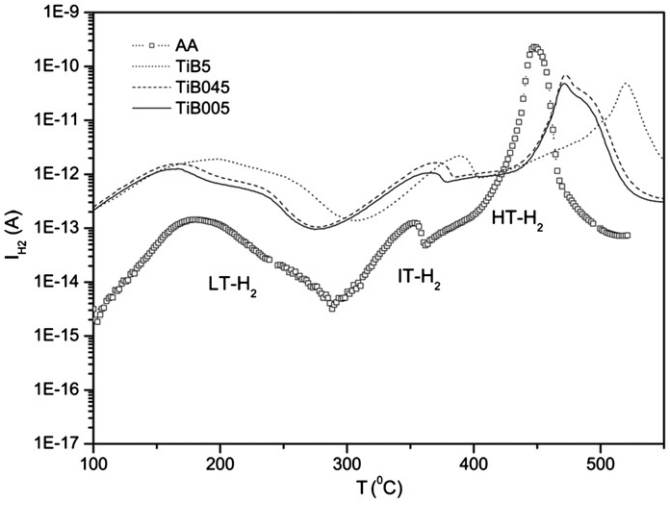

Fig. 4. TDS spectra of commercial, non-treated MgH_2 (AA) and mechanically milled composite materials: TiB5 (dot line), TiB045 (dashed line) and TiB005 (solid line). The chemical composition of composite is given in Table 1.

Having in mind the fact that the quantity of produced $Mg(OH)_2$ during the synthesis is quite high, one could say that the $MgH_2/Mg(OH)_2$ composites have been obtained during mechanical milling. Slight increase of T_{max} of HT-H_2 maxima in all composite materials can be attributed to the high quantity of hydroxide. As it was explained by Leardini et al. [30] besides the H_2O and H_2 desorption process due to $Mg(OH)_2$ dehydration and MgH_2 decomposition reactions, respectively, the solid-state reactions between MgH_2 and $Mg(OH)_2$ give rise to hydrogen desorption through another two channels. The low temperature H_2 peak (LT-H_2, $T=180$ °C) is associated to the reaction between H atom diffusing from MgH_2 and a surface OH group, whereas the intermediate temperature H_2 peak (IT-H_2 $T=350$ °C) is due to interface reaction between the hydride and the hydroxide. Quite interesting is the fact that for both TiB005 and TiB045 i.e. composites with SiC, desorption of IT-H_2 starts at lower temperature, so one can argue that SiC addition actually influences the interface reaction between hydride and hydroxide. As it can be seen from Fig. 5, the quantity of desorbed hydrogen is higher in the samples where SiC is added. Probably, the quantity of added TiB_2 in TiB5 composite was high enough to introduce negative effects on desorption capacity by blocking the H_2 diffusion paths even though the particle size of this sample is very small [16,18].

In order to investigate in detail the mechanism of MgH_2 decomposition in these samples, the shapes of the HT-H_2 desorption curves have been analyzed using different kinetic models (Fig. 6) [23]. The best fit for all samples have been obtained using the non-isothermal Avrami–Erofeev model which describes the kinetics of MgH_2 decomposition by assuming the nucleation mechanism. According to this model [23], the reacted fraction

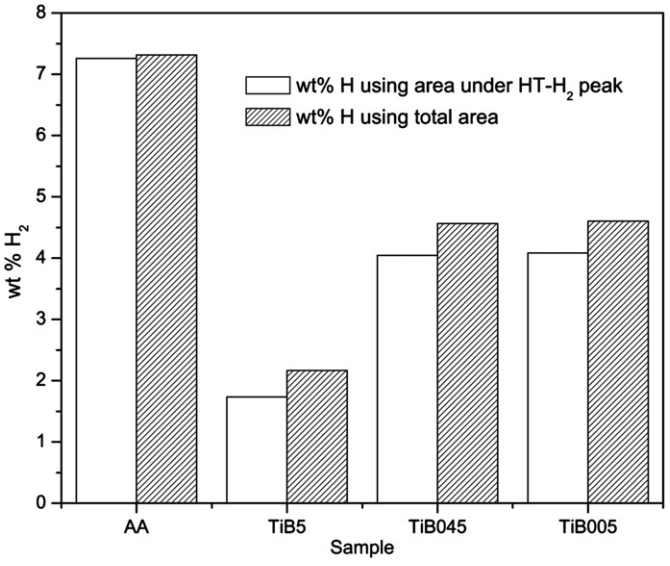

Fig. 5. Hydrogen evolution from the samples obtained using area under TDS maxima.

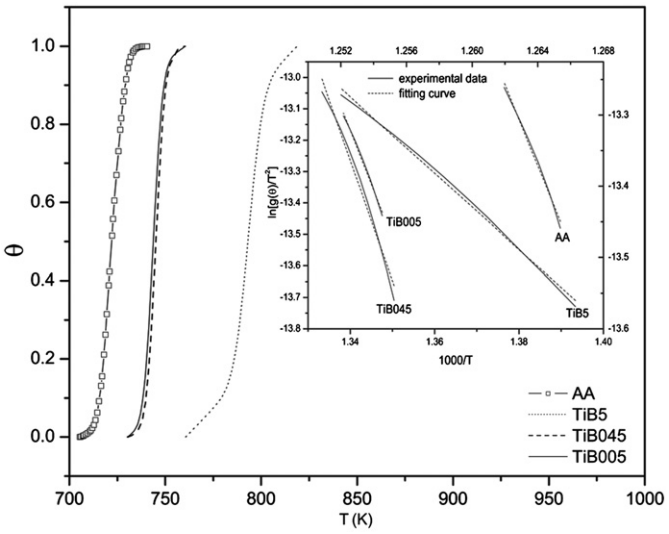

Fig. 6. Temperature evolution of the reacted fraction (θ) corresponding to MgH_2 decomposition, obtained by integration of HT-H_2 peak for commercial, non-treated MgH_2 (AA) and catalyzed samples TiB5, TiB045 and TiB005. Inset figure: from $\ln[g(\theta)/T^2]$versus $1/T$ plots, the best fit of experimental data is obtained for nucleation model (see Table 5); $g(\theta)=[-\ln(1-\theta)]^{(1/n)}$.

θ can be related to temperature (T) by:

$$\ln\left[\frac{[-\ln(1-\theta)]^{(1/n)}}{T^2}\right]=f\left(\frac{1000}{T}\right) \quad (1)$$

It can be noticed that parameter n (see Table 5) is changed from 3 (three-dimensional growth, 3D) for AA sample, into $n=4$ for all catalyzed material. Those large values discard a diffusion control and can be due to a change in the nucleation or a change in the dimensionality of the growing. Obtained activation energies, E_a (kJ/mol) of the HT-H_2 peak (Table 5) are close to values reported in the literature for MgH_2 decomposition [31–35]. The samples exposed to air exhibit very high values of parameter n, approximately 4–7 and high apparent activation energies in the order of 230–300 kJ/mol [35]. According to Varin et al. [34] the activation energy of the un-milled hydrolyzed MgH_2 is ~217 kJ/mol which can be ascribed to $Mg(OH)_2$ layer. They have also observed that even after milling in the Ar atmosphere, the values of the activation energy are still high and depend on milling time. Using *ab initio* DFT calculation Du et al. [32] estimated similar activation energy for desorption (2.86 eV–280 kJ/mol). Moreover, Hanada et al. [31] found even higher activation energy for MgH_2 desorption (323 kJ/mol). Anyhow, those values and values obtained in our research are considerably higher than those obtained by Fernández et al. (160 kJ/mol for pure MgH_2 for nucleation and growth [36]) and could be a consequence of different kinetic model used for fitting of experimental data [31] or simply a consequence of the presence of $Mg(OH)_2$ [34,35]. As it can be seen from Table 5, the activation energy for TiB_2-catalyzed MgH_2 system is considerably lower than activation energy for pure, non-treated MgH_2. Therefore, the activated surface significantly decreases the activation energy of hydrogen desorption.

Table 5
Activation energies corresponding to H_2 desorption from HT-H_2 peak obtained by the non-isothermal kinetic approach for all samples.

Sample	θ	E_a (kJ/mol)	R^{2*}	$g(\theta)=[-\ln(1-\theta)]^{(1/n)}$ (Avrami–Erofeev)
AA	0.3–0.8	276	0.996	$[-\ln(1-\theta)]^{(1/3)}$
TiB5	0.3–0.8	173	0.998	$[-\ln(1-\theta)]^{(1/4)}$
TiB045	0.3–0.8	318	0.997	$[-\ln(1-\theta)]^{(1/4)}$
TiB005	0.3–0.8	289	0.997	$[-\ln(1-\theta)]^{(1/4)}$

*R^2–correlation coefficient.

4. Conclusion

The catalytic effect of TiB_2 and SiC ceramics on desorption kinetics of MgH_2 based composites obtained by mechanical milling has been investigated by thermo-desorption spectroscopy and non-isothermal kinetic approach. The composites exhibit three desorption maxima with HT-H_2 maximum slightly moved toward higher temperatures in comparison to commercial non-treated MgH_2. This can be ascribed to increased quantity of $Mg(OH)_2$ which is formed during mechanical milling. It has been shown that TiB_2 addition leads to significant decrease of activation energy for desorption (173 kJ/mol), while SiC addition affects T_{onset} of IT-H_2 maximum, i.e. the interface reaction between hydride and hydroxide. The mechanism of H_2-desorption for all samples is Avrami–Erofeev which describes the kinetics of MgH_2 decomposition by assuming the nucleation mechanism, but the nuclei grow in different directions since parameter n changes from $n=3$ for non-treated MgH_2 to $n=4$ for composite materials.

Acknowledgment

This research was financially supported by the MEST of Serbia under Grant III 45012. We also want to express our gratitude for bilateral grant between Serbia and Spain. We are also thankful for funding to Acciones Integradas Program of Spanish MICINN through Project IB2010SE-00191. Some of us (JFF and CS) also thank Spanish MICINN for financial support under Contract MAT2011-22780.

References

[1] L. Schlapbach, A. Zuttel, Hydrogen-storage materials for mobile applications, Nature 414 (2001) 353–358.
[2] Lj. Matović, N. Novaković, S. Kurko, M. Šiljegović, B. Matović, Z. Kačarević Popović, N. Romčević, N. Ivanović, J. Grbović Novaković, Structural destabilization of MgH_2 obtained by heavy ion irradiation, International Journal of Hydrogen Energy 34 (2009) 7275–7282.
[3] J.Grbović Novaković, Lj. Matović, M. Drvendžija, N. Novaković, D. Rajnović, M. Šiljegović, Z. Kačarević Popović, S. Milovanović, N. Ivanović, Changes of hydrogen storage properties of MgH_2 induced by heavy ion irradiation, International Journal of Hydrogen Energy 33 (2008) 1876–1879.
[4] J. Huot, G. Liang, R. Schulz, Mechanically alloyed metal hydride systems, Applied Physics A 72 (2001) 187–195.
[5] F. von Zeppelin, H. Reule, M. Hirscher, Hydrogen desorption kinetics of nanostructured MgH_2 composite materials, Journal of Alloys and Compounds 330–332 (2002) 723–726.
[6] N. Hanada, T. Ichikawa, S.-I. Orimo, H. Fujii, Correlation between hydrogen storage properties and structural characteristics in mechanically milled magnesium hydride MgH_2, Journal of Alloys and Compounds 366 (2004) 269–273.
[7] V.V. Bhat, A. Rougier, L. Aymard, X. Darok, G. Nazri, J.M. Tarascon, Catalytic activity of oxides and halides on hydrogen storage of MgH_2, Journal of Power Sources 159 (2006) 107–110.
[8] J. Bellemare, J. Huot, Hydrogen storage properties of cold rolled magnesium hydrides with oxides catalysts, Journal of Alloys and Compounds 512 (2012) 33–38.
[9] J. Gulicovski, Ž. Rašković-Lovre, S. Kurko, R. Vujasin, Z. Jovanović, Lj. Matović, J. Grbović Novaković, Influence of vacant CeO_2 nanostructured ceramics on MgH_2 hydrogen desorption properties, Ceramics International 38 (2012) 1181–1186.
[10] A. Montone, J. Grbović, Lj. Stamenković, A.L. Fiorini, L. Pasquini, E. Bonetti, M.V. Antisari, Desorption behaviour in nanostructured MgH_2–Co, Materials Science Forum 518 (2006) 79–84.
[11] V.D. Dobrovolsky, O.G. Ershova, Yu.M. Solonin, O.Yu. Khyzhun, V. Paul-Boncour, Influence of TiB_2 addition upon thermal stability and decomposition temperature of the MgH_2 hydride of a Mg-based mechanical alloy, Journal of Alloys and Compounds 465 (2008) 177–182.
[12] F.J. Castro, V. Fuster, G. Urretavizcaya, Hydrogen sorption properties of a MgH_2–10 wt% graphite mixture, Journal of Alloys and Compounds 509S (2011) S595–S598.
[13] W. Oelerich, T. Klassen, R. Bormann, Comparison of the catalytic effects of V, V_2O_5, VN, and VC on the hydrogen sorption of nanocrystalline Mg, Journal of Alloys and Compounds 322 (2001) L5–L9.
[14] W. Oelerich, T. Klassen, R. Bormann, Metal oxides as catalysts for improved hydrogen sorption in nanaocrystalline Mg-based materials, Journal of Alloys and Compounds 315 (2001) 237–242.
[15] S. Kurko, Ž. Rašković, N. Novaković, B. Paskaš Mamula, Z. Jovanović, Z. Baščarević, J.Grbović Novaković, Lj. Matović, Hydrogen storage properties of MgH_2 mechanically milled with α and β SiC, International Journal of Hydrogen Energy 36 (2011) 549–554.
[16] A. Ranjbar, Z.P. Guo, X.B. Yu, D. Wexler, A. Calka, C.J. Kim, H.K. Liu, Hydrogen storage properties of MgH_2–SiC composites, Materials Chemistry and Physics 114 (2009) 168–172.
[17] H. Imamura, S. Nakatomi, Y. Hashimoto, I. Kitazawa, Y. Sakata, H. Mae, M. Fujimoto, Synthesis and hydrogen storage properties of mechanically ball-milled SiC/MgH_2 nanocomposites, Journal of Alloys and Compounds 488 (1) (2009) 265–269.
[18] A. Ranjbar, Z.P. Guo, X.B. Yu, D. Attard, A. Calka, H.K. Liu, Effects of SiC nanoparticles with and without Ni on the hydrogen storage properties of MgH_2, International Journal of Hydrogen Energy 34 (2009) 7263–7268.
[19] M.-Q. Fan, S.-S. Liu, Y. Zhang, J. Zhang, L.-X. Sun, F. Xu, Superior hydrogen storage properties of MgH_2–10 wt% TiC composite, Energy 35 (2010) 3417–3421.

[20] Y. Zhang, F. Morin, J. Huot, The effects of Ti-based additives on the kinetics and reactions in LiH/MgB_2 hydrogen storage system, International Journal of Hydrogen Energy 36 (2011) 5425–5430.
[21] M.P. Pitt, M. Paskevicius, C.J. Webb, D.A. Sheppard, C.E. Buckley, E. Mac, A. Gray, The synthesis of nanoscopic Ti based alloys and their effects on the MgH_2 system compared with the $MgH_2+0.01Nb_2O_5$ benchmark, International Journal of Hydrogen Energy 37 (2012) 4227–4237.
[22] R. Žitko, H.J.P. Van Midden, E. Zupanič, A. Prodan, S.S. Makridis, D. Niarchos, A.K. Stubos, Hydrogenation properties of the TiB_X structures, International Journal of Hydrogen Energy 36 (2011) 12268–12278.
[23] L.J. Matović, S. Kurko, Ž. Rašković-Lovre, R. Vujasin, I. Milanović, S. Milošević, J. Grbović Novaković, Assessment of changes in desorption mechanism of MgH_2 after ion bombardment induced destabilization, International Journal of Hydrogen Energy 37 (22) (2012) 6727–6732.
[24] W. Kraus, G. Nolze, PowderCell2.3 Software, Federal Institute for Materials Research and Testing (BAM), (1998).
[25] J.F. Fernández, F. Cuevas, C. Sánchez, Simultaneous differential scanning calorimetry and thermal desorption spectroscopy measurements for the study of the decomposition of metal hydrides, Journal of Alloys and Compounds 356–357 (2000) 244–253.
[26] F. Leardini, J.F. Fernández, J. Bodega, C. Sánchez, Isotope effects in the kinetics of simultaneous H and D thermal desorption from Pd, Journal of Physics and Chemistry of Solids 69 (1) (2008) 116–127.
[27] S. Milošević, Ž. Rašković-Lovre, S. Kurko, R. Vujasin, N. Cvjetićanin, Lj. Matović, J. Grbović Novaković, Influence of VO_2 nanostructured ceramics on hydrogen desorption properties from magnesium hydride, Ceramics International 39 (1) (2013) 51–56.
[28] R.A. Varin, T. Czujko, Z. Wronski, Particle size, grain size and γ-MgH_2 effects onthe desorption properties of nanocrystalline commercial magnesium hydride processed bycontrolled mechanical milling, Nanotechnology 17 (2006) 3856–3865.
[29] A. Borgschulte, U. Bosenberg, G. Barkhordarian, M. Dornheim, R. Bormann, Enhanced hydrogen sorption kinetics of magnesium by destabilized $MgH2-\delta$, Catalysis Today 120 (2007) 262–269.
[30] F. Leardini, J.R. Ares, J. Bodega, J.F. Fernández, I.J. Ferrer, C. Sánchez, Reaction pathways for hydrogen desorption from magnesium hydride/hydroxide composites: bulk and interface effects, Physical Chemistry Chemical Physics 12 (2010) 572–577.
[31] N. Hanada, T. Ichikawa, H. Fujii, Catalytic effect of nanoparticle 3D-transition metals on hydrogen storage properties in magnesium hydride MgH_2 prepared by mechanical milling, Journal of Physical Chemistry B 109 (2005) 7188–7194.
[32] A.J. Du, Sean C. Smith, X.D. Yao, G.Q. Lu, Ab initio studies of hydrogen desorption from low index magnesium hydride surface, Surface Science 600 (2006) 1854–1859.
[33] T. Kelkar, S. Pal, A computational study of electronic structure, thermodynamics and kinetics of hydrogen desorption from Al- and Si-doped α-, γ-, and β-MgH_2, Journal of Materials Chemistry 19 (2009) 4348–4355.
[34] R.A. Varin, M. Jang, T. Czujko, Z.S. Wronski, The effect of ball milling under hydrogen and argon on the desorption propertiesof MgH_2 covered with a layer of $Mg(OH)_2$, Journal of Alloys and Compounds 493 (2010) L29–L32.
[35] T.R. Jensen, A. Andreasen, T. Vegge, J.W. Andreasen, K. Stahl, A.S. Pedersen, M.M. Nielsen, A.M. Molenbroek, F. Besenbacher, Dehydrogenation kinetics of pure and nickel-doped magnesium hydride investigated by in situ time-resolved powder X-ray diffraction, International Journal of Hydrogen Energy 31 (2006) 2052–2062.
[36] J.F. Fernández, C.R. Sánchez, Rate determining step in the absorption and desorption of hydrogen by magnesium, Journal of Alloys and Compounds 340 (2002) 189–198.